First-Order Shear Horizontal Mode Resonators Design of High k_t^2 Based on $LiNbO_3$ Thin Film

Yang Li*†‡, Yushuai Liu*†‡, and Tao. Wu*†‡‡
Email: liyang12022@shanghaitech.edu.cn; liuysh2@shanghaitech.edu.cn; wutao@shanghaitech.edu.cn
*School of Information Science and Technology, ShanghaiTech University, Shanghai, China
†Shanghai Institute of Microsystem and Information Technology, Chinese Academy of Sciences, Shanghai, China
‡University of Chinese Academy of Sciences, Beijing, China
‡Shanghai Engineering Research Center of Energy Efficient and Custom AI IC, Shanghai, China

***Abstract*—In this work, high performance first-order shear horizontal (SH1) resonators with three electrode configurations based on Lithium niobate ($LiNbO_3$) thin film have been designed. The optimal Euler angle of $LiNbO_3$ and device structure are analyzed by numerical calculation and finite element analysis (FEA). A high electromechanical coupling factor (K^2) is achieved by applying double IDT electrode configuration and an electromechanical coupling coefficient (k_t^2) as high as 32.8% is achieved by optimizing normalized $LiNbO_3$ thickness, electrode coverage and normalized IDT thickness. The obtained SH1 resonators have a large k_t^2 while meeting the frequency requirement of new fifth-generation (5G) communication, which solves the disadvantage of low phase velocity of fundamental mode shear horizontal (SH0) wave based on $LiNbO_3$ thin film. This result demonstrates a first step towards introducing $LiNbO_3$ thin film based on SH1 as an alternation to SH0 mode and other traditional piezoelectric materials for 5G communication.**

Keywords—$LiNbO_3$, piezoelectric effect, SH1 resonators, 5G, electrode configuration, high k_t^2

I. INTRODUCTION

Wireless communication technology has developed rapidly in the past decades. With the swift commercialization of 5G applications [1], piezoelectric acoustic RF filters manufactured by micro-nano processing technology have been widely used in the RF front-end and various portable mobile devices due to their advantages of low cost, small size and excellent performance. Recently, resonators based on surface acoustic wave (SAW) and bulk acoustic wave (BAW) have been widely studied[2][3]. However, the performance of SAW and BAW resonator is intensively limited by the photolithography resolution and the K^2[4], which is difficult to respond the market demand for low-cost and high-performance resonators.

Compared with traditional piezoelectric materials such as aluminum nitride (AlN)[7], zinc oxide (ZnO) and lead zirconate titanate (PZT)[6], $LiNbO_3$ has a higher K^2 and quality factor Q, which meet the requirements of high frequency and broadband applications for 5G communication[7]. Thus shear horizontal (SH) wave resonator based on $LiNbO_3$, which is generated by using IDT and propagating in the thin film[8], is selected in this paper.

Among various SH mode, SH0 resonator based on $LiNbO_3$ thin film has demonstrated a novel k_t^2 of more than 50%, but its phase velocity is not high (4800 m/s)[9], which causes many difficulties in high frequency applications. Therefore, an elastic wave with high velocity is required to use in $LiNbO_3$ thin film. SH1 mode has a higher phase velocity, which meets the needs of 5G communication[10]. Although the K^2 of the SH1 mode is lower than that of the fundamental mode, SH1 mode still have an excellent K^2 theoretically comparing with other acoustic mode, which is sufficient to meet the need of driving efficiency of RF resonators.

In this work, numerical calculation on the maximum K^2 for exciting SH1 in rotated Y-cut $LiNbO_3$ thin-film and in-plane orientation is carried out, so as to obtain the optimal Euler angle parameters under Lateral Field Excited (LFE) and Thickness Field Excited (TFE) conditions[11]. The authors also have explored different thickness of $LiNbO_3$ thin film to achieve high frequency and high k_t^2 SH1 resonators under three types of electrode configuration. The structure with single IDT, IDT/floating BE and double IDT electrode layout theoretically has a high k_t^2, which is much higher than that of traditional piezoelectric materials while having a high resonance frequency. However, there are some spurious modes coupling into the SH1 mode, which will introduce annoying ripples in the passband when building filters using these resonators. After making some compromises on performance, a spurious free SH1 resonator with relative high k_t^2 is obtained. Finally, the admittance diagram under the optimal device structure and electrode configuration is presented.

Yang Li and Yushuai Liu are equal contribution

2022 IEEE International Ultrasonics Symposium (IUS) | 978-1-6654-6657-8/22/$31.00 ©2022 IEEE | DOI: 10.1109/IUS54386.2022.9957283

II. STRUCTURAL OPIMIZAION

A. Numerical Calculation of Euler Angle

Fig. 1 shows the cross-sectional illustrations for the electric potentials and electric fields with three electrode configurations in one-port of $LiNbO_3$ resonator under one voltage electric potential. The three electrode configurations are single IDT, IDT/floating BE and double IDT, which are named as Type A, Type B and Type C, respectively[12]. If the edge electric field is ignored, then Type A is LFE condition and the electric field direction is 1 (x direction). Similarly for Type B and Type C, they are both TFE condition and the electric field direction is 3 (z direction).

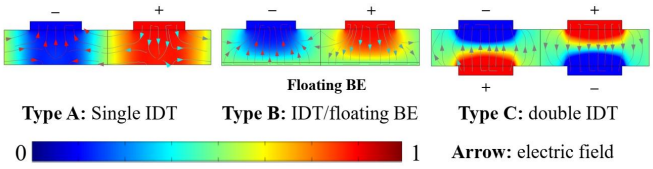

Fig. 1. Three types of electrodes configurations for exciting SH1 mode, cross-sectional illustrations of the electric potentials and electric fields in one-port $LiNbO_3$ resonators.

Piezoelectric materials will transform energy from mechanical domain into electrical domain when subjected to stress, or transform energy from electrical domain into mechanical domain when subjected to electric field. The K^2, which represents the ability of piezoelectric materials to transform energy in two domains, is an inherent property of materials, independent of external excitation and topological structure. When h_{LN} is smaller than the wavelength λ, it can be defined and estimated as[13]:

$$K_{ij}^2 = \frac{e_{ij}^2}{\varepsilon_{ii}^T c_{jj}^E} \approx \frac{f_0^2 - f_m^2}{f_0^2} \quad (1)$$

where i represents the direction of the electric field, j represents the direction of mechanical stress, e_{ij} is the piezoelectric stress constant in the direction of the electric field i and mechanical stress j, ε_{ii}^T is permittivity in the direction of electric field i at zero stress, c_{jj}^E is elastic stiffness in the direction of mechanical stress j at zero electric field, v_0 is the phase velocity of free boundary condition, v_m is the phase velocity of metallized condition, f_0 is the resonant frequency and f_m is the anti-resonance frequency. Since $LiNbO_3$ is an anisotropic material, the optimal Euler angle needs to be determined through numerical calculation to obtain the highest K^2. The Euler angle transformation in this article is based on the Z-X-Z rotation with the Euler angles of (α, β, γ), where $\gamma = 0°$, α is propagation angle and also known as in plane orientation angle, 90°-β represent rotated cutting angle when $\gamma = 0°$ and $0° < \beta < 90°$(270°-β represent rotated cutting angle when $\gamma = 0°$ and $90° < \beta < 180°$).

To make the resonator work efficiently, the Euler angle with high K^2 is highly demanded. SH1 is excited by T_{yz} (stress of 4 direction), which means that the optimal Euler angle needs to be determined to obtain a high K_{14}^2 or K_{34}^2. For the same piezoelectric material, ε_{ii}^T and c_{jj}^E are constant matrix, so K_{14}^2 and K_{34}^2 is proportional to e_{14}^2 and e_{34}^2. Fig. 2 illustrates the calculated maximum piezoelectric coefficient e_{14} and e_{34} for exciting SH1 in rotated Y-cut $LiNbO_3$ thin-films and maximum K^2 in-plane orientation under LFE and TFE conditions when β is fixed at the optimal value. As shown in Fig. 2, for type A electrode configuration, there is a maximum piezoelectric coefficient for 2.57 C/m^2 at rotated 145° Y-cut (β = -55°) with K_{14}^2 is up to 30.05% at α = 48°. For type B and type C electrode configuration, there is a maximum 3.89 C/m^2 for piezoelectric coefficient at rotated 170° Y-cut (β = -80°) and K_{34}^2 is up to 67.16% at α = 0°. The FEM simulation in the following will be based on the optimal rotated cutting angle and propagation angle obtained in this section.

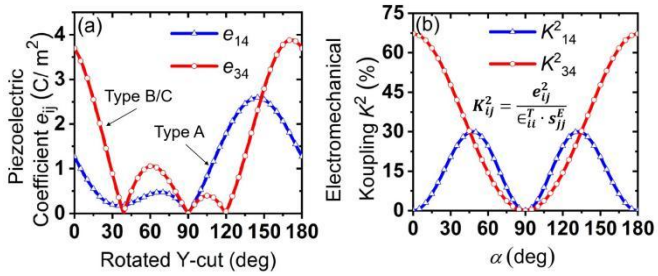

Fig. 2. Calculated maximum piezoelectric coefficient for exciting SH1 in rotated Y-cut $LiNbO_3$ thin-films and maximum K^2 in-plane orientation under LFE and TFE conditions.

B. Optimization of Device Structure by FEM Simulations

The surface of $LiNbO_3$ has two boundary conditions (B.C.): free B.C. and metallized B.C., which can be combined into three situations when considering both upper and lower surface of $LiNbO_3$ thin film: both upper and lower surface are free B.C., upper surface is metalized B.C. and lower surface is free B.C., both upper and lower surface are metalized B.C.. For type A electrode configuration, resonant frequency (f_0) can be obtained by simulating the SH1 Eigen mode of $LiNbO_3$ thin film with both upper and lower surface are free B.C., anti-resonant frequency (f_m) can be obtained by simulating the SH1 Eigen mode of $LiNbO_3$ thin film with upper surface is metalized B.C. and lower surface is free B.C.. Similarly, for type B electrode configuration, f_0 can be obtained by simulating the SH1 eigen mode of $LiNbO_3$ thin film with upper surface is free B.C. and lower surface is metalized B.C., f_m can be obtained by simulating the SH1 eigen mode of $LiNbO_3$ thin film with both upper surface and lower surface is metalized B.C.. For type C electrode configuration, f_0 can be obtained by simulating the SH1 eigen mode of $LiNbO_3$ thin film with both upper and lower surface are free B.C., f_m can be

obtained by simulating the SH1 eigen mode of $LiNbO_3$ thin film with both upper and lower surface are metalized B.C.. The K^2 of the three electrode structures can be obtained by substituting f_0 and f_m into formula 1 respectively[14].

To optimize the device structure, first, the normalized $LiNbO_3$ thickness: h_{LN}/λ of SH0 mode and SH1 mode is scanned parametrically from 0.05 to 0.3 where h_{LN} is the thickness of $LiNbO_3$ which is fixed to 1 μm and λ is the wavelength of SH1 mode. Simultaneously, same simulation is performed on Type A, Type B and Type C electrode configuration. As shown in Fig. 3(a) that with the decrease of h_{LN}/λ, phase velocity of SH1 mode increases exponentially while SH0 mode remains almost unchanged. Fig. 3(b) illustrates the variation relationship between K^2 and h_{LN}. Considering both phase velocity and K^2, the best normalized $LiNbO_3$ thickness for Type A, Type B and Type C is 0.05, 0.2 and 0.2, respectively.

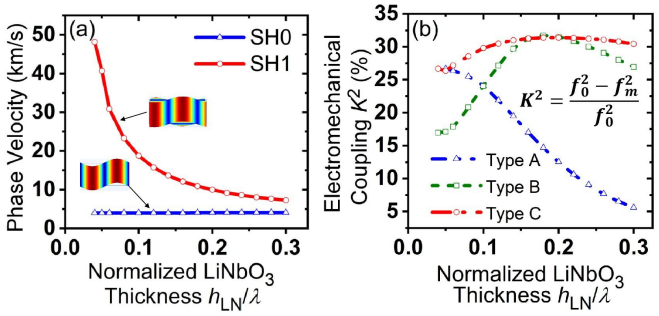

Fig. 3. Dispersion curve of (a) Phase velocity and (b) K^2 under different h_{LN}/λ.

Electrodes coverage is defined as: $E_c = S_{IDT}/S_{LN}$, where S_{IDT} is the upper surface area of IDT and S_{LN} is the upper surface area of $LiNbO_3$. Parametrical scanning is performed on E_c under the optimal normalized $LiNbO_3$ thickness of Type A, Type B and Type C electrode configurations respectively. As shown in Fig. 4(a), the best electrodes coverage for Type A, Type B and Type C is 0.4, 0.5 and 0.5, respectively.

Similar to h_{LN}/λ, the normalized metal electrode thickness: h_{IDT}/λ of Type A, Type B and Type C electrode configurations are scanned parametrically from 0 to 0.04 in the case of optimal normalized $LiNbO_3$ thickness and electrodes coverage. As shown in Fig. 4(b), Type A, Type B and Type C has the theoretical maximum k_t^2 up to 25.3%, 29.3% and 32.8% when the normalized metal electrode thickness is 0.026, 0.034 and 0.024, respectively. As shown in Fig. 4(b) that Type A electrode configuration is more sensitive to the changes of h_{IDT}/λ than Type B and Type C electrode configuration. This is because the K^2 of Type B and C electrode configurations as TFE condition is more than twice that of Type A electrode configuration as LFE condition when all structures are at the optimal Euler angle, as shown in Fig. 2. This makes both Type B and Type C electrode configurations to have better potential against the changes of IDT thickness which is independent from $LiNbO_3$ thin film.

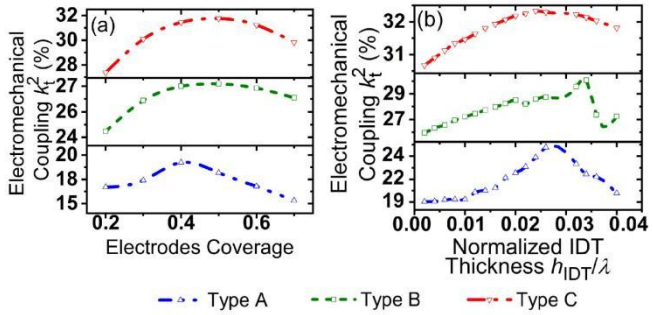

Fig. 4. Simulated k_t^2 of type A/B/C electrode configurations under different E_c and h_{IDT}/λ.

Unfortunately, the special ion cutting process of $LiNbO_3$ thin film makes it difficult to realize this electrode configuration by a more economical and reliable method[15]. What's more, there are some spurious mode near the resonance peak, which will create annoying ripples in the passband of filters composed of these resonators[16][17]. By adjusting the device structure, part of k_t^2 is sacrificed in exchange for a spurious free SH1 resonator.

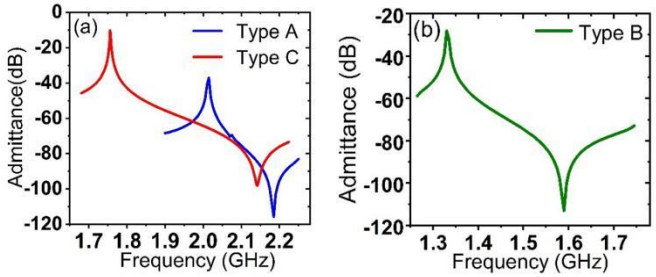

Fig. 5. Simulated admittance of spurious free design with (a) Type A, Type C and (b) Type B electrode configurations.

To sum up, the authors propose the SH1 mode resonators in different electrodes configurations to obtain high phase velocity and high k_t^2. For type A electrode configuration, a large k_t^2 of 17.5% can be achieved when h_{LN}/λ = 0.13, h_{IDT}/λ = 0.007 and electrodes coverage is 0.4 based on (48°, -55°, 0°) $LiNbO_3$ thin film. For type B electrode configuration, a large k_t^2 of 29% can be achieved when h_{LN}/λ = 0.125, h_{IDT}/λ = 0.034 and electrodes coverage is 0.5 based on (0°, -80°, 0°) $LiNbO_3$ thin film. For type C electrode configuration, a large k_t^2 of 32.8% can be achieved when h_{LN}/λ = 0.18, h_{IDT}/λ = 0.024 and electrodes coverage is 0.5 based on (0°, -80°, 0°) $LiNbO_3$ thin film. The admittance diagrams of the three electrode configurations under the best k_t^2 device structure are drawn as shown in Fig. 5. The final spurious free device structure still have a relatively high k_t^2 after making a compromise on performance.

III. CONCLUSION

In this work, rotated cutting angle and propagation angle of $LiNbO_3$ under LFE and TFE conditions were numerically calculated to obtain the optimal Euler angle parameters. After that, the piezoelectric thin film thickness, electrode coverage and electrode thickness of the device under the three electrode configurations are simulated parametrically and optimized by FEM. Finally, a spurious free SH1 resonator based on $LiNbO_3$ thin film exhibits a novel performance of high k_t^2 (32.8%) and a suitable f_0 (1.76 GHz) has been achieved.

ACKNOWLEDGMENT

This work was supported in part by the National Natural Science Foundation of China under Grant 61874073, and in part by the Lingang Laboratory under Grant LG-QS-202202-05.

REFERENCES

[1] P. Popovski, K. F. Trillingsgaard, O. Simeone, and G. Durisi, "5G Wireless Network Slicing for eMBB, URLLC, and mMTC: A Communication-Theoretic View," IEEE Access, vol. 6, pp. 55765–55779, 2018, doi: 10.1109/ACCESS.2018.2872781.

[2] M. Kadota and S. Tanaka, "Solidly mounted resonator using shear horizontal mode plate wave in LiNbO3 plate," 2016 IEEE International Frequency Control Symposium (IFCS), 2016, pp. 1-4, doi: 10.1109/FCS.2016.7546795.

[3] P. Kirsch, M. B. Assouar, O. Elmazria, V. Mortet, and P. Alnot, "5GHz surface acoustic wave devices based on aluminum nitride/diamond layered structure realized using electron beam lithography," Appl. Phys. Lett., vol. 88, no. 22, p. 223504, May 2006, doi: 10.1063/1.2208372.

[4] P. Kirsch, M. B. Assouar, O. Elmazria, V. Mortet, and P. Alnot, "5GHz surface acoustic wave devices based on aluminum nitride/diamond layered structure realized using electron beam lithography," Appl. Phys. Lett., vol. 88, no. 22, p. 223504, May 2006, doi: 10.1063/1.2208372.

[5] A. Ballato, "Piezoelectricity: old effect, new thrusts," IEEE Trans. Ultrason. Ferroelectr. Freq. Control, vol. 42, no. 5, pp. 916–926, Sep. 1995, doi: 10.1109/58.464826.

[6] J. D. III, S. R. Gilbert, and B. Xu, PZT Material properties at UHF and microwave frequencies derived from FBAR measurements, vol. 1. 2004, p. 177 Vol.1. doi: 10.1109/ULTSYM.2004.1417696.

[7] S. Gong and G. Piazza, "Design and Analysis of Lithium–Niobate-Based High Electromechanical Coupling RF-MEMS Resonators for Wideband Filtering," IEEE Trans. Microw. Theory Tech., vol. 61, no. 1, pp. 403–414, Jan. 2013, doi: 10.1109/TMTT.2012.2228671.

[8] F. Setiawan, M. Kadota and S. Tanaka, "SH1Mode Plate Wave Resonator on LiTaO3 Thin Plate with Phase Velocity over 13,000 m/s," 2021 IEEE International Ultrasonics Symposium (IUS), 2021, pp. 1-4, doi: 10.1109/IUS52206.2021.9593629.

[9] Y. Liu, K. Liu and T. Wu, "Design and Analysis of High kt2 Shear Horizontal Wave Resonators," 2021 IEEE International Ultrasonics Symposium (IUS), 2021, pp. 1-4, doi: 10.1109/IUS52206.2021.9593617.

[10] M. Kadota, S. Tanaka and T. Kimura, "First shear horizontal mode plate wave in LiNbO3 showing 20 km/s phase velocity," 2015 IEEE International Ultrasonics Symposium (IUS), 2015, pp. 1-4, doi: 10.1109/ULTSYM.2015.0458.

[11] R. Lu and S. Gong, "RF acoustic microsystems based on suspended lithium niobate thin films: advances and outlook," J. Micromechanics Microengineering, vol. 31, no. 11, p. 114001, Nov. 2021, doi: 10.1088/1361-6439/ac288f.

[12] J. Zou et al., "Design of Ultra-Large-Coupling SH 0 Plate Wave Resonators on LiNbO 3 with Clean Spectrum," in 2019 Joint Conference of the IEEE International Frequency Control Symposium and European Frequency and Time Forum (EFTF/IFC), Orlando, FL, USA, Apr. 2019, pp. 1–6. doi: 10.1109/FCS.2019.8856043.

[13] Tsung-Tsong Wu and Yung-Yu Chen, "Exact analysis of dispersive SAW devices on ZnO/diamond/Si-layered structures," in IEEE Transactions on Ultrasonics, Ferroelectrics, and Frequency Control, vol. 49, no. 1, pp. 142-149, Jan. 2002, doi: 10.1109/58.981392.

[14] Zou, Jie. "High quality factor Lamb wave resonators." EECS Department University of California, Berkeley Technical Report No. UCB/EECS-2014-217 (2014).

[15] L. Shao et al., "Microwave-to-optical conversion using lithium niobate thin-film acoustic resonators," Optica, vol. 6, no. 12, p. 1498, Dec. 2019, doi: 10.1364/OPTICA.6.001498.

[16] J. Kaitila, "3C-1 Review of Wave Propagation in BAW Thin Film Devices - Progress and Prospects," in 2007 IEEE Ultrasonics Symposium Proceedings, New York, NY, Oct. 2007, pp. 120–129. doi: 10.1109/ULTSYM.2007.43.

[17] T. Wu, Y. Wong, Y. He, C. Peng, J. Bao, and K. Hashimoto, "Spurious-free thickness-shear bulk acoustic resonators on lithium niobate using standard and broadband piston mode designs," Jpn. J. Appl. Phys., vol. 61, no. 2, p. 025503, Feb. 2022, doi: 10.35848/1347-4065/ac42ae.